

Resolution Enhancement in Electron-Nuclear Double Resonance through Multiple-Quantum Transitions

N. S. Dalal

National Research Council, Ottawa K1A 0R9, Canada

and

A. Manoogian

Department of Physics, University of Ottawa, Ottawa K1N 6N5, Canada

(Received 19 September 1977)

The identification of multiple-quantum transitions and their utilization in enhancing the resolution of electron-nuclear double-resonance (ENDOR) spectra are described. It is shown that for $^{53}\text{Cr}^{3+}$ ions substituted in hydrated crystals the linewidths of double-quantum ENDOR transitions are an order of magnitude smaller than those of the normal ENDOR transitions.

The electron-nuclear double-resonance (ENDOR) technique has proven to be a powerful method for investigating paramagnetism in solids and liquids. The main advantage of ENDOR over standard electron-spin resonance (ESR) is the higher spectral resolution obtained. In ENDOR experiments one usually detects NMR transitions through their effect on the intensity of an inhomogeneously broadened ESR transition. The improvement in resolution corresponds to the ratio of the width of the ESR line to the width of a spin packet, which is one of the components comprising the ESR line. Although this method usually yields a resolution enhancement of two to three orders of magnitude, a further increase in resolution should be obtainable if multiple-quantum NMR transitions can be detected, i. e., when two or more rf photons combine to produce a given transition. Time-dependent perturbation theory shows that the linewidth of an n -quantum transition should be $1/n$ of the corresponding single-quantum transition.¹ Thus the linewidth of a double-quantum transition ($n=2$) should be approximately half that of a single-quantum transition for the same set of energy levels. This reduction in linewidth has been seen in molecular-beam,² ESR,³ and NMR spectroscopy,⁴⁻⁷ and in the present work we report on the observation and identification of double- and triple-quantum transitions in the ENDOR spectra of $^{43}\text{Cr}^{3+}$ substituted as a dilute impurity in alums. The only other work related to such features in the ENDOR spectra is a reference to "extra lines" observed by Danilov and Manoogian.⁸ These lines are identified in the present work as double-quantum transitions, but it is found that their linewidths are an order of magnitude smaller than the allowed lines, rather than just a factor of 2.

The double- and triple-quantum transitions were studied in the $^{53}\text{Cr}^{3+}$ ENDOR spectra of CsAl and RbAl sulfate alums at 4.2 K using a spectrometer described previously.⁸ The only modification was the use of a 20-W rf power amplifier rather than the previous 3-W unit. In either case, however, only a portion of the power entered the two-turn ENDOR coil, because of mismatch. The rf power was frequency modulated at 405 Hz and deviations from 1 to 25 kHz were used.

The magnetic resonance spectra of the $^{53}\text{Cr}^{3+}$ ($3d^3$) ion in alums have been well characterized by the spin Hamiltonian^{8,9}

$$\mathcal{H} = \mu_B \vec{H} \cdot \vec{g} \cdot \vec{S} + \vec{S} \cdot \vec{D} \cdot \vec{S} + \vec{I} \cdot \vec{A} \cdot \vec{S} \\ + \vec{I} \cdot \vec{Q} \cdot \vec{I} - \mu_N \vec{H} \cdot \vec{g}_N' \cdot \vec{I},$$

where $S = I = \frac{3}{2}$, and the terms have their usual meaning. The ESR fine-structure spectrum consists of three allowed ($\Delta M_s = \pm 1$) transitions with a separation of $2D$ between adjacent lines for $H \parallel z$, where z is the crystallographic $[111]$ direction. Each fine-structure line is further split into a 1:1:1:1 quartet by the ^{53}Cr hyperfine interaction $\vec{I} \cdot \vec{A} \cdot \vec{S}$. The quadrupole interaction $\vec{I} \cdot \vec{Q} \cdot \vec{I}$ is not resolved in ESR but has been studied in detail through ENDOR.^{8,9} The fine-structure energy level diagram for CsAl alum is shown in Fig. 1. The insets in the figure show the hyperfine splittings and positions of the observed ENDOR transitions. The allowed transitions ($\Delta M_s = 0$, $\Delta M_I = \pm 1$) are labeled 1, 3, and 5, and those of the double-quantum transitions as 2 and 4. The position of the triple-quantum transition nearly coincides with the central allowed transition 3.

A typical ENDOR spectrum obtained in CsAl with $H \parallel z$, and H_z set at an arbitrary position in

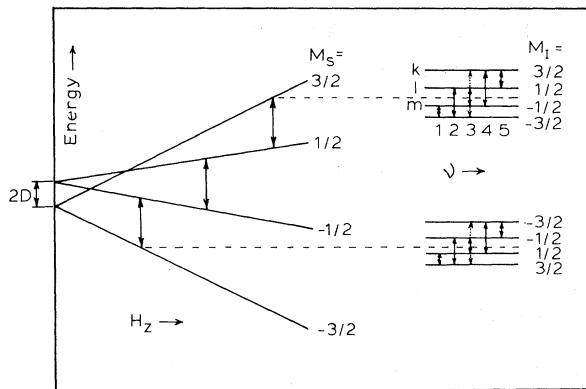


FIG. 1. Fine-structure energy level diagram of $^{53}\text{Cr}^{3+}$ in CsAl alum with $H \parallel z$. Insets show the hyperfine splittings (not to scale) with observed ENDOR transitions.

the $M_s = \frac{3}{2}$ hyperfine manifold, is shown for low rf power (< 1 W) in Fig. 2(a), and for relatively high power (~ 3 W) in Fig. 2(b). Figure 2(c) shows an expanded-scale spectrum of the triple-quantum transition superimposed on the central allowed transition at the highest rf power (~ 4 W). The triple-quantum line has low intensity at the rf power levels used. A list of the measured ENDOR line positions for CsAl and RbAl alums for $M_s = \pm \frac{3}{2}$ and $H \parallel z$ is given in Table I. The intensities of the double-quantum transitions in the $M_s = -\frac{3}{2}$ state for CsAl alum were much reduced compared to those of the $M_s = \frac{3}{2}$ state, with only a trace of them being observable. This effect can be explained by considering the theory governing ENDOR line intensity ratios. Well-resolved double-quantum transitions were obtained in RbAl alum for both the $M_s = \pm \frac{3}{2}$ states.

Transitions 2 and 4 are identified as double-

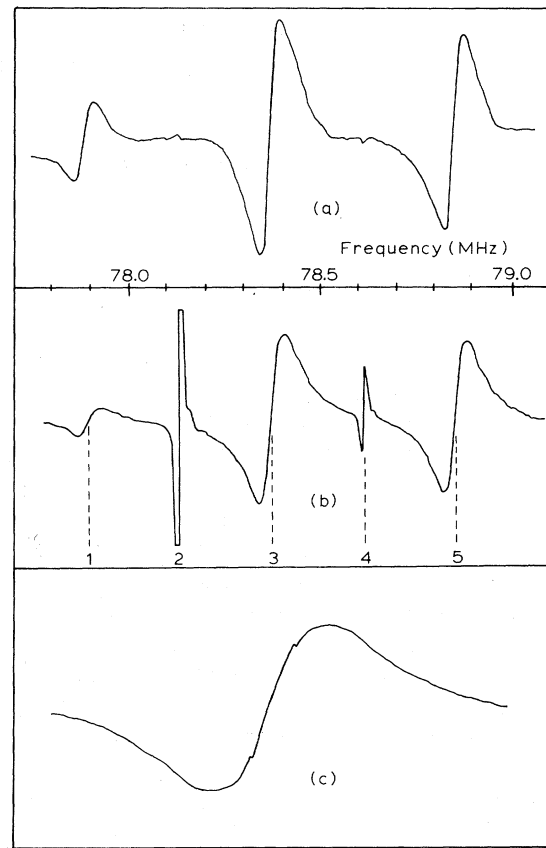


FIG. 2. $^{53}\text{Cr}^{3+}$ ENDOR spectra in CsAl alum for $M_s = \frac{3}{2}$ and $H \parallel z$. H_z is set at an arbitrary position within the hyperfine manifold. (a) Allowed transitions 1, 3, and 5 at low rf power (< 1 W). (b) Allowed lines plus the double-quantum transitions marked 2 and 4 at relatively high rf power (~ 3 W). (c) Expanded spectrum of the triple-quantum transition superimposed on the central allowed line at maximum rf power (~ 4 W).

quantum ENDOR transitions on the basis of the following observations. The intensity ratio of a

TABLE I. ENDOR frequencies (MHz) of $^{53}\text{Cr}^{3+}$ in Cs and Rb aluminum alums for $H \parallel z$.

	CsAl alum		RbAl alum	
	$M_s = 3/2$	$M_s = -3/2$	$M_s = 3/2$	$M_s = -3/2$
Magnetic field, H_z (T)	0.4934	0.1830	0.2604	0.4112
Transition				
1	77.899	75.548	77.971	77.030
2	78.135		78.249	77.184
3	78.368	77.190	78.525	77.336
4	78.610		78.804	77.487
5	78.854	78.548	79.087	77.642
$(\omega_{1k} - \omega_{mk}/2)^{-2}$				
$M_I = 3/2 \rightarrow -1/2$	16.95	2.20	13.04	44.44
$M_I = 1/2 \rightarrow -3/2$	18.25	2.17	12.67	42.74

double-quantum transition (I_{dq}) to that of a single-quantum transition (I_{sq}) is given by second-order time-dependent perturbation theory¹⁰ as

$$\frac{I_{dq}}{I_{sq}} = \frac{1}{2} \left(\frac{g\beta}{\hbar} \right)^2 \left(\frac{H_{rf}}{\omega_{lk} - \frac{1}{2}\omega_{mk}} \right)^2 \frac{\Delta\nu_{kl}}{\Delta\nu_{km}} |\langle l|S_+|k\rangle|^2, \quad (1)$$

where k , l , and m refer to three adjacent energy levels, as marked in Fig. 1. The chief characteristics of Eq. (1) are these: (a) The resonance frequency ν_{km} of a double-quantum transition is given by $\nu_{km} = \frac{1}{2}(\nu_{kl} + \nu_{lm})$; (b) the intensity ratio I_{dq}/I_{sq} depends linearly on $|H_{rf}|^2$, which is proportional to the power in the ENDOR coil; (c) $I_{dq}/I_{sq} \propto (\omega_{lk} - \frac{1}{2}\omega_{mk})^{-2}$; and (d) the linewidth of the double-quantum transition $k \rightarrow m$ ($\Delta\nu_{km}$) is at least one-half of the linewidth of the transition $k \rightarrow l$ ($\Delta\nu_{kl}$). All these characteristics are found to hold for the transitions 2 and 4.

Point (a) can be verified from the list of frequencies in Table I. Point (b) was verified by studying the ENDOR signals at variable rf power levels. These results are presented in Fig. 3 for the $M_s = \frac{3}{2}$ state of CsAl alum. At lower power levels, where Eq. (1) is valid, the linear dependence is satisfied. Point (c) was similarly verified for the transition frequencies listed in Table I. For example, the relatively small value of the factor $(\omega_{lk} - \frac{1}{2}\omega_{mk})^{-2}$ for the $M_s = -\frac{3}{2}$ state of CsAl alum accounts well for the near failure to detect double-quantum transitions in that state. Finally, the reduction in linewidth of the double-quantum transitions is clearly seen in Fig. 2(b). The minimum linewidths occur at an FM deviation of approximately 5 kHz.

The peak-to-peak linewidths of the double-quantum ENDOR transitions are only 8 ± 2 kHz, compared to 80 ± 5 kHz for the normal ENDOR lines. The extra reduction (by a factor of 5) is tentative-

ly attributed to the fact that the linewidths of the normal lines have a dominant contribution due to a slight spread in quadrupole interaction from crystal imperfections. The double-quantum transitions will be largely unaffected by such effects, as can be noted from recent NMR studies.^{7,11} In this respect we feel that multiple-quantum transitions should be helpful in extending the elegant ENDOR-enhanced NMR technique introduced by Kwiram and co-workers.¹² The double-quantum transitions may be particularly useful in developing this method for higher-resolution NMR studies. In analogy with the NMR studies,^{7,11} they may also be useful for resolving deuteron chemical shifts, particularly in powders. If successful, the use of ENDOR will result in an increase in the sensitivity over NMR methods by two to three orders of magnitude.

In summary, we believe that in many cases for $I > \frac{1}{2}$, or for equivalent nuclei with $I = \frac{1}{2}$, double-quantum transitions should be observable in ENDOR experiments using moderate rf power, and that the linewidths of these transitions will be substantially smaller than those of the corresponding normal ENDOR signals. At higher power levels the triple-quantum transitions can also be detected and these may yield even sharper features. The observation of multiple-quantum ENDOR transitions for $^{53}\text{Cr}^{3+}$ in hydrated crystals is expected to be quite general since they were also observed during the course of this work in single crystals of guanidinium aluminum sulfate hexahydrate. These transitions were not observed in the previous ENDOR study of this crystal¹³ because of severe line broadening caused by the large FM deviation used (75 kHz). It is possible that this effect may also be the case in other ENDOR studies where other factors fa-

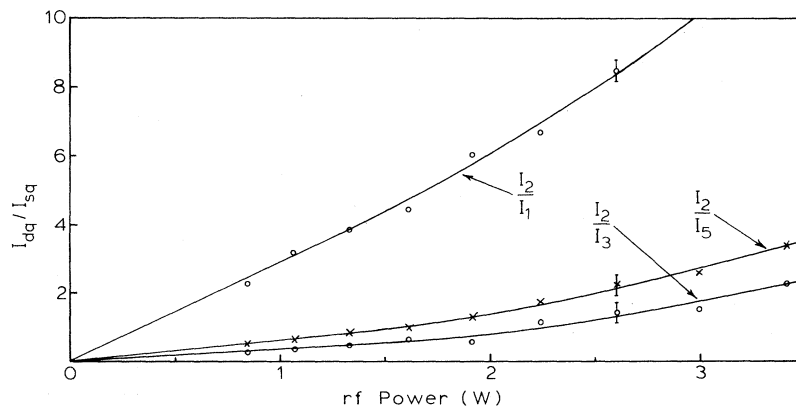


FIG. 3. Intensity ratios I_{dq}/I_{sq} as a function of rf power for the transitions 1, 2, 3, etc. of Fig. 2(b).

vor the observation of the multiple-quantum transitions.

¹See, for example, V. W. Hughes and J. S. Geiger, Phys. Rev. **99**, 1842 (1955), and references therein.

²V. W. Hughes and L. Grabner, Phys. Rev. **79**, 828 (1950).

³For recent references see A. Carrington *et al.*, J. Chem. Phys. **47**, 4859 (1967); C. A. McDowell and I. Tanaka, Chem. Phys. Lett. **26**, 463 (1974).

⁴W. Anderson, Phys. Rev. **104**, 850 (1955).

⁵R. C. Hewitt, S. Meiboom, and L. C. Snyder, J. Chem. Phys. **58**, 5089 (1973); L. C. Snyder and S. Meiboom, J. Chem. Phys. **58**, 5096 (1973).

⁶R. E. McDonald and T. K. McNab, Phys. Rev. Lett. **32**, 1133 (1974), and references therein, for double-quantum transitions in depolarization-detected NMR

transitions.

⁷A. Pines, D. J. Reuben, S. Vega, and M. Mehring, Phys. Rev. Lett. **36**, 110 (1976), and references therein.

⁸A. G. Danilov and A. Manoogian, Phys. Rev. B **6**, 4103 (1972).

⁹A. Manoogian and B. Auger, Can. J. Phys. **52**, 1731 (1974).

¹⁰S. A. Al'tshuler and B. M. Kozyrev, *Electron Paramagnetic Resonance* (Academic, New York, 1964), p. 87.

¹¹S. Vega, T. W. Shattuck, and A. Pines, Phys. Rev. Lett. **37**, 43 (1976).

¹²R. C. McCalley and A. L. Kwiram, Phys. Rev. Lett. **24**, 1279 (1970); A. L. Kwiram and L. R. Dalton, J. Am. Chem. Soc. **94**, 6930 (1972).

¹³A. Manoogian and A. Leclerc, Phys. Rev. B **10**, 1052 (1974).

Photoelectron Spectra of Hydrogenated Amorphous Silicon

B. von Roedern, L. Ley, and M. Cardona

Max-Planck-Institut für Festkörperforschung, 7000 Stuttgart 80, Federal Republic of Germany

(Received 25 August 1977)

uv-induced and x-ray-induced photoelectron spectra have been taken on hydrogenated amorphous silicon prepared *in situ* by reactive sputtering. Hydrogen-induced features in the *a*-Si valence-band region have been identified by comparison with spectra and calculations appropriate to the adsorption of hydrogen onto Si surfaces. Films sputtered at room temperature show peaks related to Si multiply bonded to hydrogen, while deposition at 300°C or above is mainly causing the formation of singly bonded SiH groups.

When hydrogen is incorporated into amorphous silicon (*a*-Si) either by preparing films from a glow-discharge plasma of silane¹ (SiH₄) or by reactively sputtering the material in an Ar-H₂ mixture,^{2,3} the dangling bonds believed to be present at the inner surfaces of microvoids or multivacancies are saturated by hydrogen atoms attached to them.⁴ This conjecture is supported by the reduction in the electron-spin-resonance signal^{5,7} and the presence of Si-H vibrational modes observed in the infrared absorption.^{7,8} The presence of hydrogen is therefore essential for the substitutional doping of *a*-Si either by glow discharge⁹ or by sputtering techniques,¹⁰ which has enabled the construction of solar cells based on *a*-Si.¹¹ This exciting possibility has triggered an increasing number of investigations on the electronic and transport properties of *a*-Si with H concentrations that exceed those necessary to merely saturate dangling bonds.^{3,8} In this Letter we report the photoemission spectra of *a*-Si with varying degrees of hydrogenation. The H-induced additional structure in the *a*-Si valence band can

be explained by an incorporation of H into the *a*-Si network, the main configurations being SiH and SiH₃. These results have been derived by comparing our spectra with experiments and calculations of H chemisorbed on Si single-crystal surfaces. A reduction in width of the Si valence band up to 1 eV suggests a partial destruction of the Si network for H concentrations in excess of approximately 10%.

Photoelectron spectra of *a*-Si:H were measured with a resolution of 0.3 eV using He I (21.2 eV) and He II (40.8 eV) radiation for the valence-band region, while Al K α (1486.6 eV) x rays were employed to obtain core-level spectra at a resolution of 1.1 eV.

The samples were prepared *in situ* (base pressure 1×10^{-9} Torr) by dc sputtering from a single-crystal Si target (50 Ω cm, *n* type, 18 mm diam) in a mixture of Ar and H₂. Depending on the deposition temperature T_D , substrates of Cu ($T_D > 300^\circ\text{C}$) or W ($T_D > 300^\circ\text{C}$) were used. The distance between target and substrate was about 4 cm, and the deposition angle was 45°. The sput-